AN296279, Rev. 1
MCO-0001356
P0241

MAGNET DESIGN GUIDELINES FOR A33020/A33023 STRAY FIELD IMMUNE ANGLE SENSOR

By Yannick Vuillermet
Allegro MicroSystems

INTRODUCTION

The A33020 and A33023 are 360° angle sensor ICs that provide contactless high-resolution, high-accuracy angular position information based on magnetic sensing technology. The A33020 is a system-on-chip (SoC) architecture that includes angle sensing, digital signal processing, and various output options: SPI, PWM, motor commutation (U,V,W), and encoder outputs (A, B, I). Also integrated in the device is on-chip EEPROM technology, capable of supporting a high number of read/write cycles for flexible end-of-line programming of calibration parameters. The A33020 is qualified to AEC-Q100 grade 0.

The A33020 is based on Hall-effect technology. It is capable of rejecting common mode DC stray field up to 50 G and AC stray field according to ISO11452-8 Test Level IV, due to its patented concept of six Hall elements placed in a circle.

The A33020 is an absolute angular position sensor designed for end-of-shaft configuration (Figure 1). A rotating permanent magnet is placed in front of the A33020. The magnetic field generated by the magnet are sensed by the Hall elements of the A33020: the corresponding signals are converted to an angle position by internal digital signal processing circuits.

This application note gives guidelines on permanent magnet selection based on application requirements: air gap, placement tolerances, magnet shape, etc.

Note that this application note also applies to the A33022.

KEY DEFINITIONS

The A33020 has six planar Hall plates equally spaced in a 2.0 mm diameter circle (Figure 2). Three differential channels CHA, CHB, and CHC are created out of these six Hall plates:

- CHA = HP1 – HP4
- CHB = HP2 – HP5
- CHC = HP3 – HP6

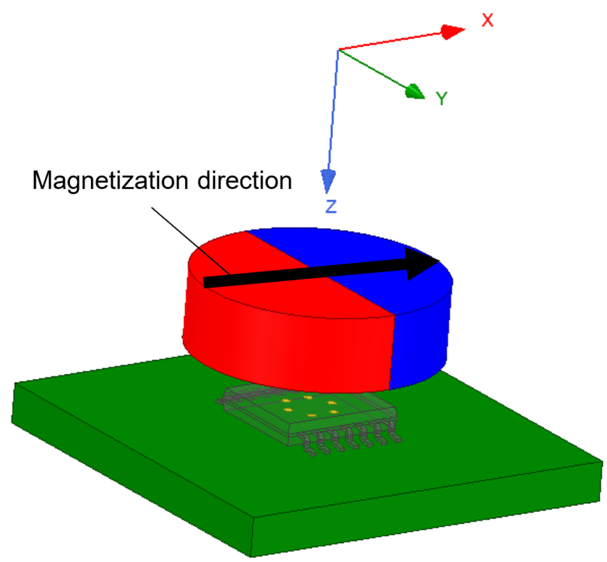

Figure 1: Angle sensing, End of Shaft configuration, Diametrical magnetization

HPi is the magnetic field measured by the Hall plate i along the direction Z, perpendicular to the surface of the chip.

Two composite field magnitudes are of interest: the "Input Magnetic Flux Density" B_{IN}, and the "Differential Input Magnetic Flux Density" ΔB.

The "Input Magnetic Flux Density" B_{IN} is defined below in equation 1.

Equation 1:

$$B_{IN} = \frac{1}{3} \times \sqrt{\left(\frac{\sqrt{3}}{2}(CH_B + CH_C)\right)^2 + \left(CH_A + \frac{1}{2}(CH_B - CH_C)\right)^2}$$

This input field B_{IN} reflects the signal strength within the main angle sensing channel (the combined magnitude of all three channels) and defines the actual resolution of the system: the higher B_{IN}, the better the resolution.

The "Differential Input Magnetic Flux Density" ΔB is defined below in equation 2.

Equation 2:

$$\Delta B = \frac{1}{2} \times \max\left(|CH_A|, |CH_B|, |CH_C|\right)$$

It corresponds to half the maximum absolute value of any of the three differential channels. It is scaled down (ratio ½) to be consistent with B_{IN} (as a single-ended field).

Note that, by definition, with the A33020 perfectly centered over a cylindrical magnet diametrically magnetized, B_{IN} is equal to the maximum single-ended field over a 360° rotation (Figure 3 and Figure 4).

Equation 3:

$$B_{IN} = \max(\Delta B) = \max(HPi) \quad \text{with } i = 1{:}6$$

Finally, the output angular noise Δφ is given by equation 4.

Equation 4:

$$\Delta\varphi = \frac{k}{B_{IN}}$$

where Δφ is the 1-sigma noise in degrees and k is a value dependent on the front-end configuration of the IC. Typical values of k are reported in Table 1. The "-300" and "-600" identifier in the part numbers for the A33020/A33023 indicate a factory-programmed sensitivity range for the part (Table 2). Note that the "-300" part number has less angle noise then "-600", at a given input field B_{IN}. However, "-600" can handle higher B_{IN} and ΔB (ΔB < 400 G for "-300" part number and ΔB < 600G for "-600"part number).

Table 1

k	"-300" Part Number			"-600" Part Number		
Temperature	–40°C	25°C	150°C	–40°C	25°C	150°C
BW = 6.25 kHz	5	5	11	9	9	13
BW = 12.5 kHz	7	7	16	12	12	18
BW = 25 kHz	9	9	18	14	14	22
BW = 50 kHz	11	11	24	19	19	29

Table 2

Part Number	System Die	Target Magnet Field Range
A33020LLEATR-300	Single	200 to 400 G
A33020LLPBTR-DD-300	Dual	200 to 400 G
A33020LLEATR-600	Single	300 to 600 G
A33020LLPBTR-DD-600	Dual	300 to 600 G

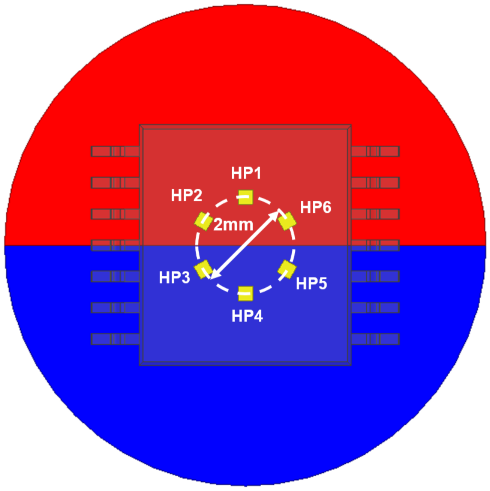

Figure 2: Hall plates definition

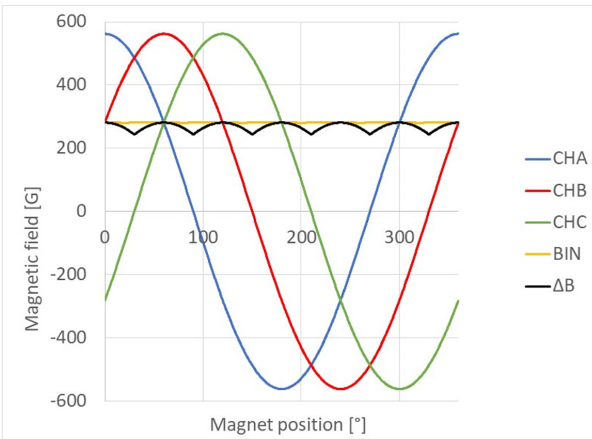

Figure 3: Example of A33020 key fields and differential channels, over 360° magnet rotation, with cylindrical magnet, diametrical magnetization, and ideal magnet placement versus the IC

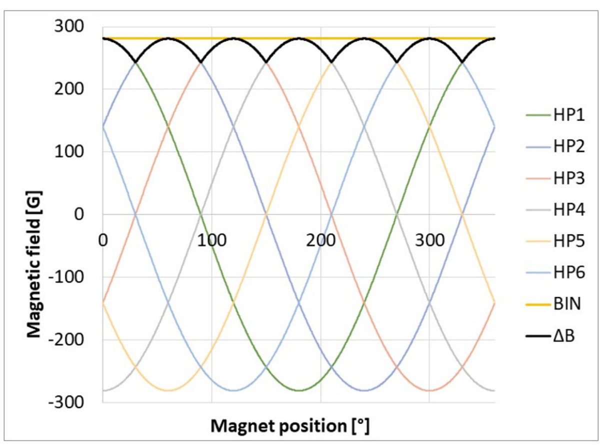

Figure 4: Example of A33020 key fields and single ended fields, over 360° magnet rotation, with cylindrical magnet, diametrical magnetization, and ideal magnet placement versus the IC

Crystal air gap is defined from the A33020 Hall elements to the top of the magnet (Figure 5). Package air gap is the distance between the package to the top of the magnet. Finally, "aad" stands for "active area depth" and is defined in equation 5.

Equation 5:

$$Crystal\ air\ gap = Package\ air\ gap + aad$$

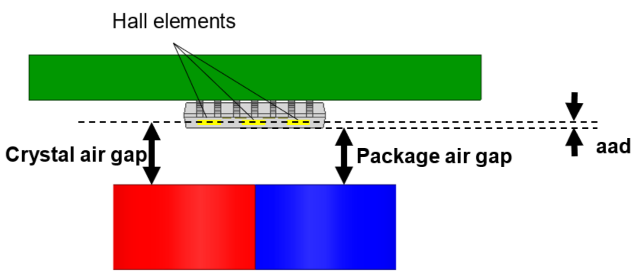

Figure 5: Air gap definition

MAGNET DESIGN GUIDELINES

A large range of magnet dimensions and shapes can be used with A33020. While a four-pole axial magnetization (Figure 6) works with A33020, it is recommended to use a diametrical magnetization; for the same performances, a diametrically magnetized magnet is considerably lighter, less bulky and costly.

The general flowchart to assist the magnet design is shown in Figure 7. The flowchart starts with an initial magnet design that can be derived from the mappings shown in the next section and appendix. Next, the magnetic field HPi induced by the magnet at the six Hall plate positions is simulated with a magnet strength Br = 1 T, and for any placement tolerances and tilt of the A33020 versus the magnet. The corresponding input magnetic flux density B_{IN} and ΔB are derived from the HPi. The maximum differential input magnetic flux density ΔB_{max} must be calculated based on the application requirements derived in equation 6:

Equation 6:

$$\Delta B_{max} = \max\left(\Delta B \times Br_{max}\right)$$

Br_{max} is the maximum magnet strength of the application magnet material, at the minimum application temperature. Equation 7 derives the magnet strength Br at a temperature T, given the magnet strength at 20°C and the temperature coefficient α (given as a percentage).

Equation 7:

$$B_r(T) = B_r(20°) \times \left(1 + \frac{\alpha}{100}(T - 20)\right)$$

If ΔB_{max} is greater than the datasheet maximum value of ΔB, then the magnet is too strong. The induced magnetic field must be reduced by using a smaller magnet or by using a weaker magnet material. Otherwise, the minimum B_{IN_min} field is calculated based on equation 8.

Equation 8:

$$B_{IN\_min} = \min\left(B_{IN} \times Br_{min}\right)$$

Br_{min} is the minimum magnet strength of the application magnet material, at the maximum application temperature and including lifetime loss, if any. The corresponding maximum angle noise in the application is calculated with equation 4. If the application angle noise and the inherent angle accuracy (also sometimes called non-linearity due to eccentricity) requirements are met, then the magnet suits the application. Otherwise, the magnet needs to be enlarged or stronger magnet material should be considered.

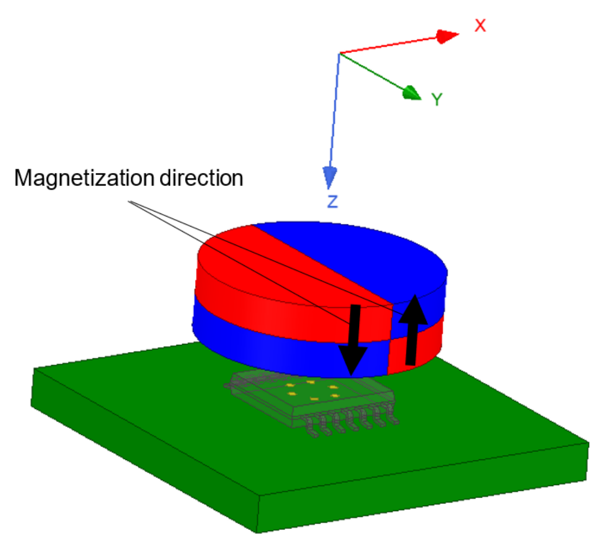

Figure 6: Four poles axial magnetization, cylindrical magnet

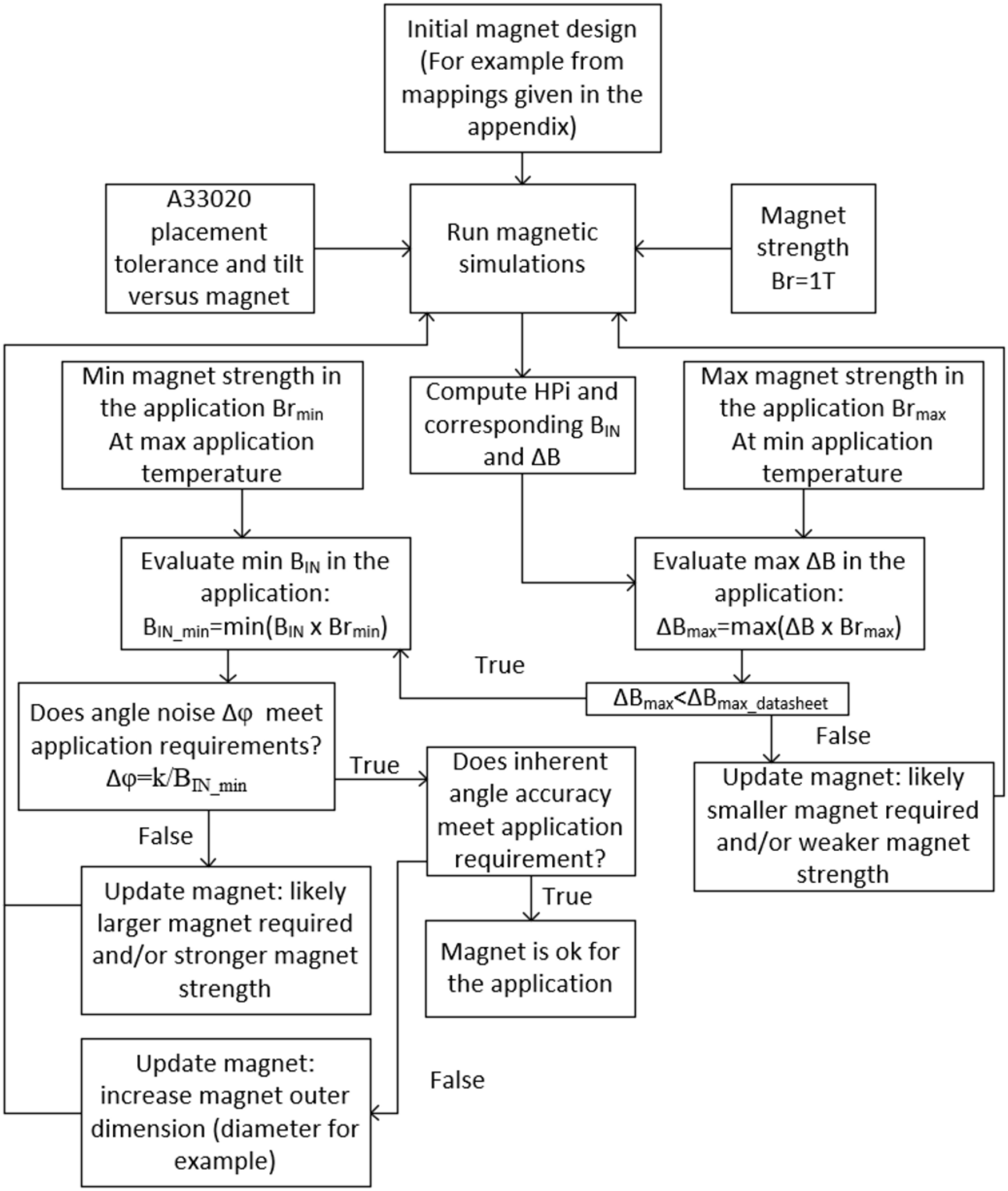

Figure 7: Magnet design flowchart

MAGNET MAPPINGS EXAMPLE

A full set of magnet mappings, or lookup tables, are available in the Appendix 1 for a cylindrical magnet with a diametrical magnetization (Figure 8), and in the Appendix 2 for a square magnet with magnetization along one side (Figure 9). Other magnet shapes (block, cylindrical with one or more cut sides, etc.) should also perform well with the A33020, if designed according to the recommended flowchart (Figure 7).

The first type of mapping (Figure 14 and Figure 17; see appendix) returns the maximum value of ΔB, using Br = 1 T and over 360° rotation, versus the magnet dimensions and for various crystal air gaps. It assumes the A33020 is perfectly centered in front of the magnet. Note that all results are given versus crystal air gap; this figure is more convenient when working with devices that have different active area depths aad.

The second type of mappings (Figure 15, Figure 16, Figure 18, and Figure 19; see appendix) represents the inherent maximum angular error over 360° rotation due to an in-plane misalignment between the A33020 and the magnet. These mappings assume there is no ferromagnetic material around the sensor, for example, a shaft that holds the magnet. If there is any ferromagnetic material near the sensor, the mappings cannot be used. In this case, magnetic simulations can be run to generate results.

In the following section, only some subsets, with 2 mm crystal air gap, are used to exhibit the results; see Figure 10 (for cylindrical magnets) and Figure 11 (for square magnets). First, the differential input magnetic field ΔB is very similar between the square and the cylindrical shapes. To generate the greatest ΔB, the outer magnet dimension (OD or X) should be less than 10 mm. ΔB also increases with greater magnet height H. Regarding accuracy, it is not recommended to use very small values of OD or X, for example less than 6 mm, because they induce the highest angular errors for a given placement tolerance. A cylindrical magnet tends to generate less angular error, compared to a square magnet, with a sweet spot where non-linearity is basically zero. In Figure 10, the sweet spot slightly depends on OD and H but it is generally around OD = 9 mm. However, Figure 15 shows that the sweet spot varies with air gap. There is no sweet spot with the square magnet: the angular error is independent on the magnet height H and only decreases with greater X.

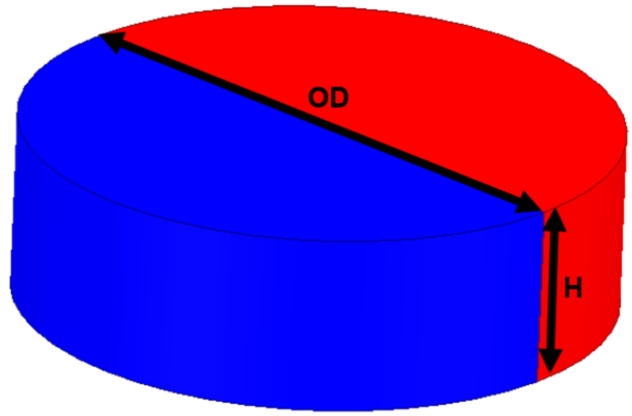

Figure 8: Cylindrical magnet dimensions

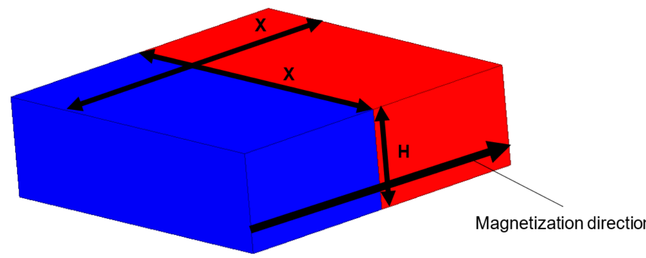

Figure 9: Square magnet dimensions and magnetization orientation

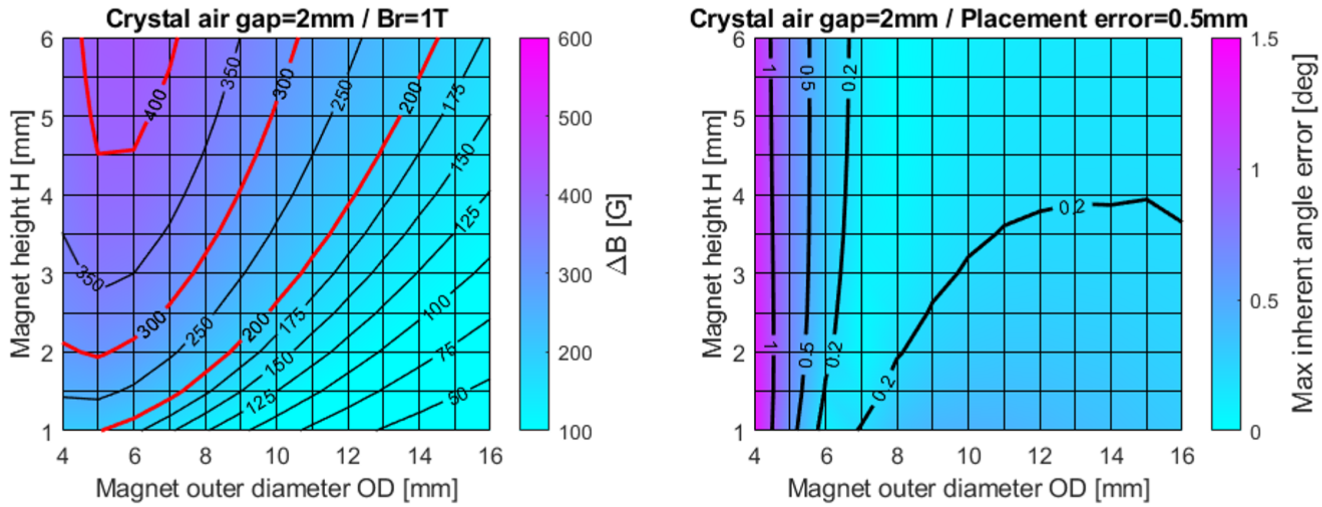

Figure 10: Cylindrical magnet, ΔB with Br = 1 T and ideal A33020 placement versus the magnet (left) and Maximum angle error over 360° with 0.5 mm in-plane A33020 misplacement versus the magnet (right)

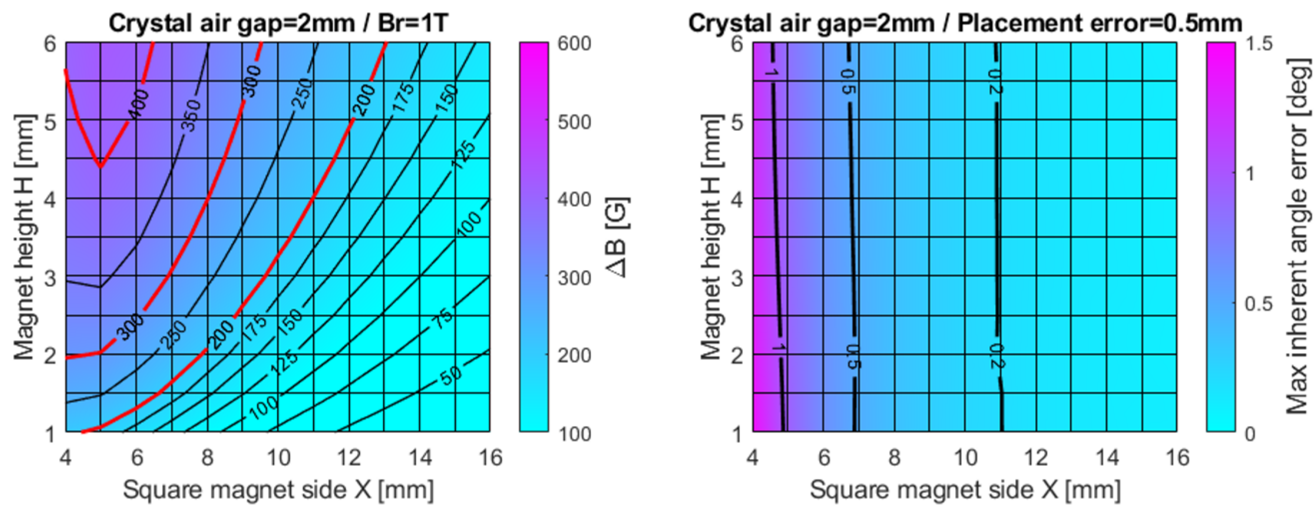

Figure 11: Square magnet, ΔB with Br = 1 T and ideal A33020 placement versus the magnet (left) and Maximum angle error over 360° with 0.5 mm in-plane A33020 misplacement versus the magnet (right)

MAGNET DESIGN EXAMPLE

In this section, the initial magnet design selection of flowchart from Figure 7 is explained. The application has the following requirements:

- Cylindrical magnet with diametrical magnetization
- Ambient temperature: –40°C to 150°C
- Magnet strength at 20°C: Br varies from 0.70 T to 0.73 T (lifetime loss included)
- Magnet temperature coefficient: –0.03%/°C
- Package air gap: 1.8mm ±0.5mm
- Placement tolerance in-plane: ±0.5mm
- Maximum angular noise: 0.1° 1-sigma with BW = 25 kHz
- 360° rotation
- No ferromagnetic material in the vicinity of the sensor
- Single die version: from the datasheet, the corresponding area depth is aad = 0.33 mm

Breaking down the process into several steps:

1. Calculate field strength required to meet resolution requirement:

Based on equation 4, the minimum B_{IN} is 18/0.1 = 180 G (using "-300" part number). With 10% margin, to account for misplacement, it gives $B_{IN} \geq 200$ G.

2. Calculate minimum magnet strength at the maximum ambient temperature:

The maximum ambient temperature for this application is,150°C, calculating the magnet strength at this temperature using equation 7: $Br_{min} = 0.7 \times [1 - 0.03 / 100 \times (150 - 20)] = 0.67$ T.

3. Determine magnet dimensions using maps provided in the Appendix

The mappings in the appendix were generated for Br = 1 T. To scale the plots to match the application magnet the values within the map should be multiplied by 0.67 (the minimum magnet strength calculated in step 2). After scaling, the 300 G contour line equates to 201 G, conveniently close to the targeted B_{IN} for this application (200 G as determined in step 1). Next the maximum crystal air gap in the application must be determined. Adding together the nominal air gap, tolerance, and active area depth results in a value of 2.63 mm (1.8 + 0.5 + 0.33), aligning closely to the 2.5 mm air gap of Figure 14 and Figure 15. The relevant plots are reminded in Figure 12.

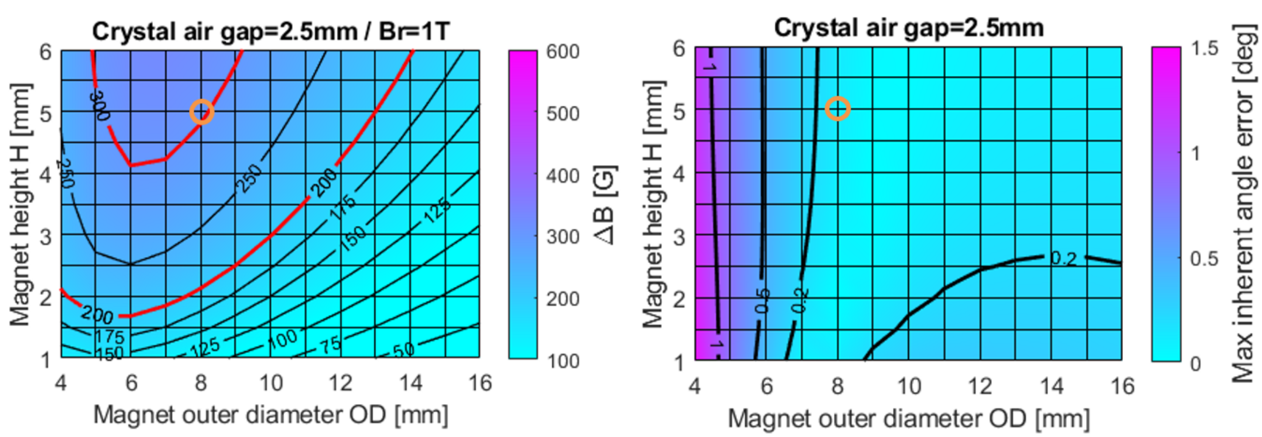

Figure 12: Field and Error Maps for 2.5 mm air gap. Orange circle shows a possible magnet size option.

Examining the two maps for an air gap of 2.5 mm show that a magnet size of OD = 8 mm and H = 5 mm should meet the system requirements (see orange circles in figure above); with an estimated non-linearity of less than 0.2°. Another possibility magnet size is OD = 6 mm / H = 4 mm. This meets the magnetic field requirement and requires less magnetic material; however results in larger angle error over misalignment (≈0.5° instead of 0.2°).

4. Calculate field strength at the minimum ambient temperature and minimum air gap

At –40°C the calculated Br_{max} (using equation 7) is: 0.73 × [1 – 0.03 / 100 × (–40 – 20)] = 0.74 T. The minimum crystal air gap is 1.63 mm (1.8 – 0.5 + 0.33). Looking again to Figure 14 (relevant excerpt is in Figure 13), this time using the 1.5 mm air gap plot, shows a magnet of OD = 8 mm / H = 5 mm results in ≈420 G. Scaling this by 0.74 results in a field of ≈310 G, below the maximum 400 G field for a "-300" part number.

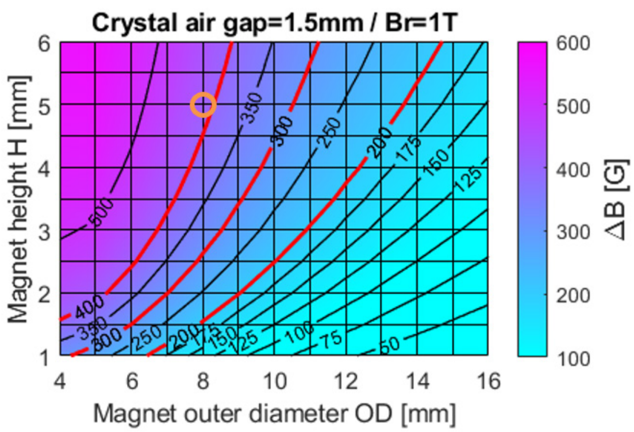

Figure 13: Field Map for air gap of 1.5 mm. Orange circle shows a possible magnet size option magnet size.

The flowchart from Figure 7 can now be run with a magnet size of OD = 8 mm and H = 5 mm to check if B_{IN} and ΔB are in the expected range, over all placement tolerances and tilts.

Note that "-600" part number is not recommended in this specific application. The minimum B_{IN} would be 23/0.1 = 230 G. With 10% margin to account for misplacement, it gives $B_{IN} \geq$ 250 G. The minimum magnet strength is still 0.67 T. Since, the mappings in appendix 1 are given for Br = 1 T, the targeted B_{IN} for this application is 250/0.67 ≈ 370 G. This value is not in the mappings of Figure 14 for 2.5mm crystal air gap. Using "-600" would require an exaggeratedly bulky magnet.

ALLEGRO A33020 REFERENCE MAGNETS

Allegro recommends the cylindrical magnets below for two use cases regarding crystal air gap and placement tolerances.

This table is valid for:

- 360° rotation
- No ferromagnetic material in the vicinity of the sensor
- Cylindrical magnet with diametrical magnetization
- –40 to 150°C
- SmCo magnet:
    - Magnet strength at 20°C: Br varies from 1.00 T to 1.03 T (lifetime loss included)
    - Magnet temperature coefficient: –0.03%/°C

These magnets can be, for example, found at ShinEtSu (http://www.shinetsu-rare-earth-magnet.jp/e/) or Bomatec (https://www.bomatec.com/en/).

CONCLUSIONS

The A33020 performs well in front of a variety of magnets over a wide range of tolerances, if the magnet is properly designed. This application note focuses on cylindrical and square based magnets, but other shapes (rectangle based, cylindrical with cuts, etc.) can also be used to achieve good performance. It is recommended to use a magnet with its magnetization orthogonal to the axis of rotation (such as a diametrical magnetization for a cylindrical magnet). The results in this application note show the best accuracy performances are obtained with a cylindrical magnet.

Allegro engineers can assist in designing the optimum magnet for a specific application.

Contact an Allegro representative for any further questions or support.

Table 3

#	OD (mm)	H (mm)	Crystal Air Gap (mm)	Part Number	Placement Tolerance	Minimum B_{IN} (G)	Maximum ΔB (G)	Volume (mm^3)
1	7	2	1.5	300	±0.5 mm in all directions ±3° tilt in all directions	250	380	77
2	10	4	2	300	±1.0 mm in all directions ±3° tilt in all directions	200	350	315
3	6	3	1.5	600	±0.5 mm in all directions ±3° tilt in all directions	330	600	84
4	8	6	2	600	±1.0 mm in all directions ±3° tilt in all directions	245	575	302

Appendix 1: Cylindrical Magnet Mapping, with Diametrical Magnetization

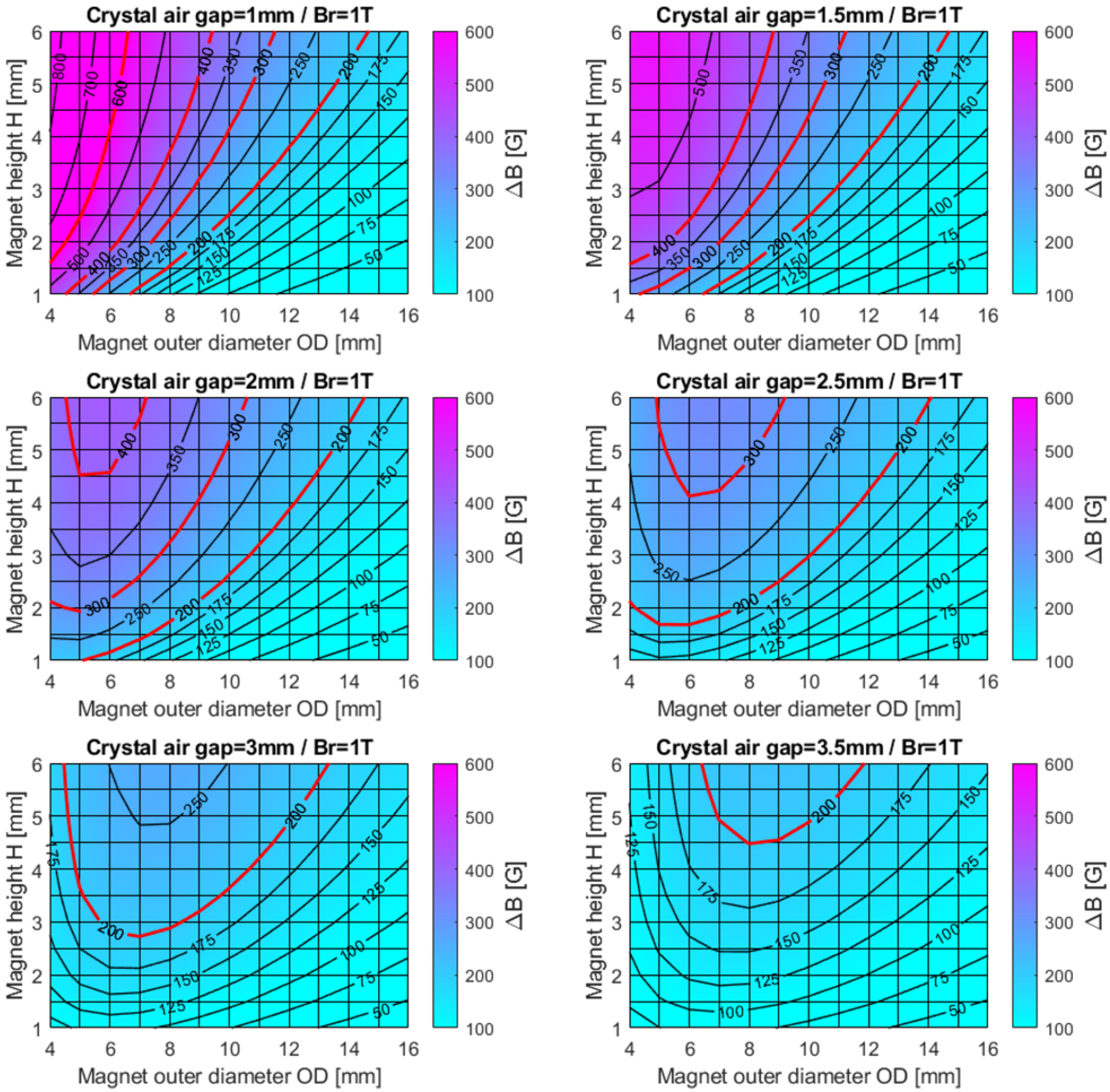

Figure 14: Cylindrical magnet, Differential input magnetic flux density with Br = 1 T and ideal A33020 placement versus the magnet

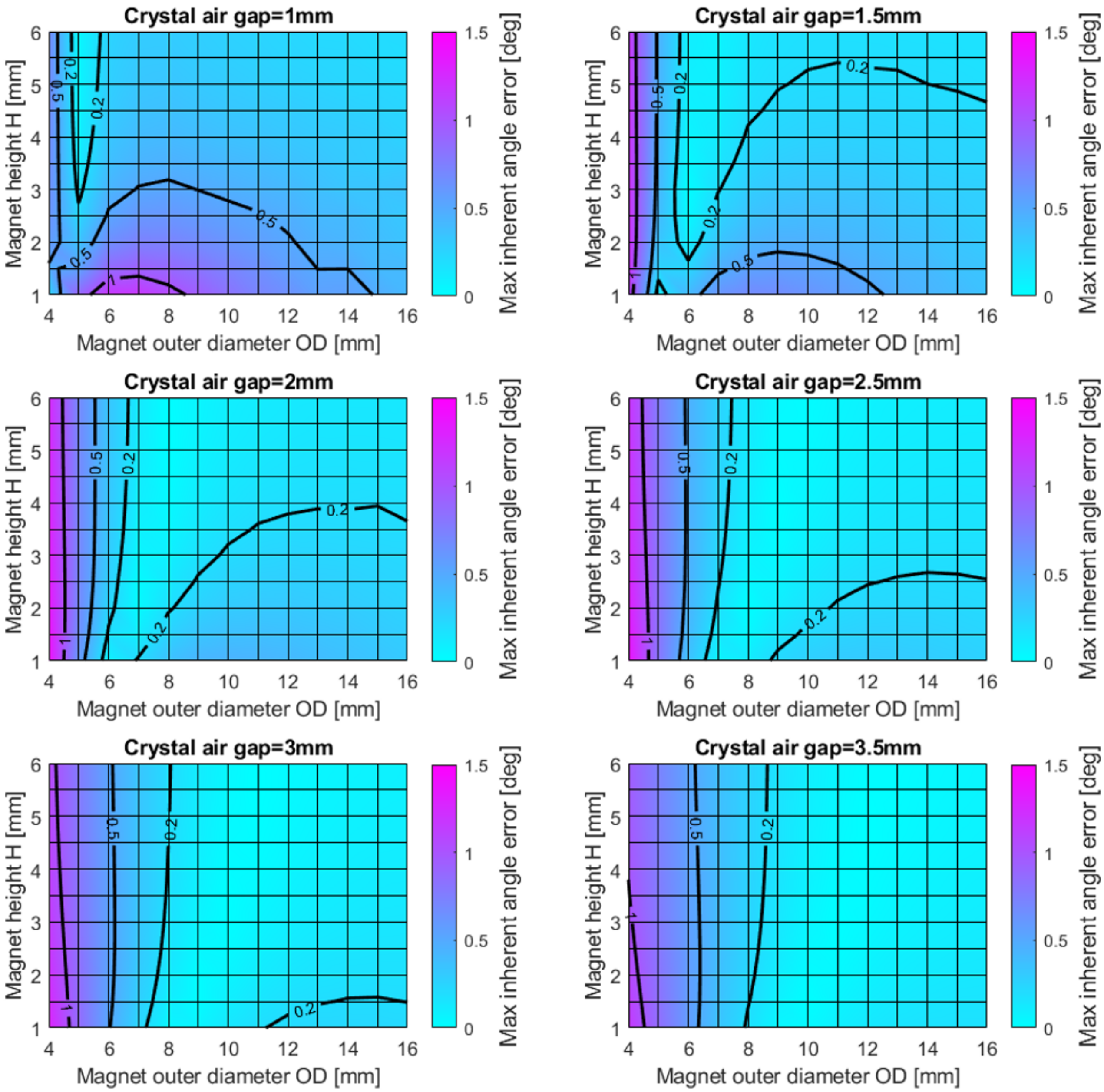

Figure 15: Cylindrical magnet, Maximum angle error over 360° with 0.5 mm in-plane A33020 misplacement versus the magnet

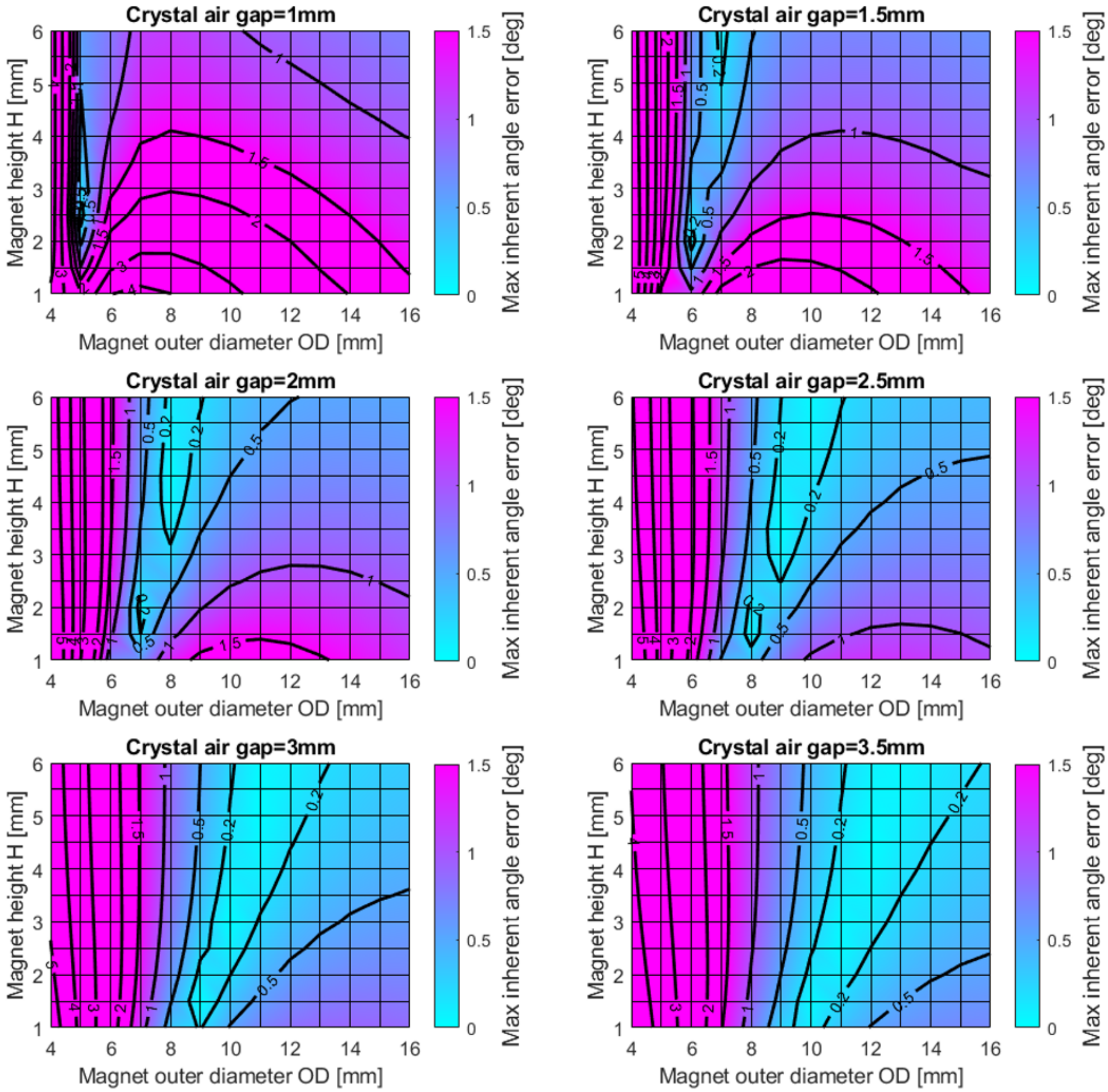

Figure 16: Cylindrical magnet, Maximum angle error over 360° with 1.0 mm in-plane A33020 misplacement versus the magnet

Appendix 2: Square Magnet Mapping, Magnetization Along One Square Side

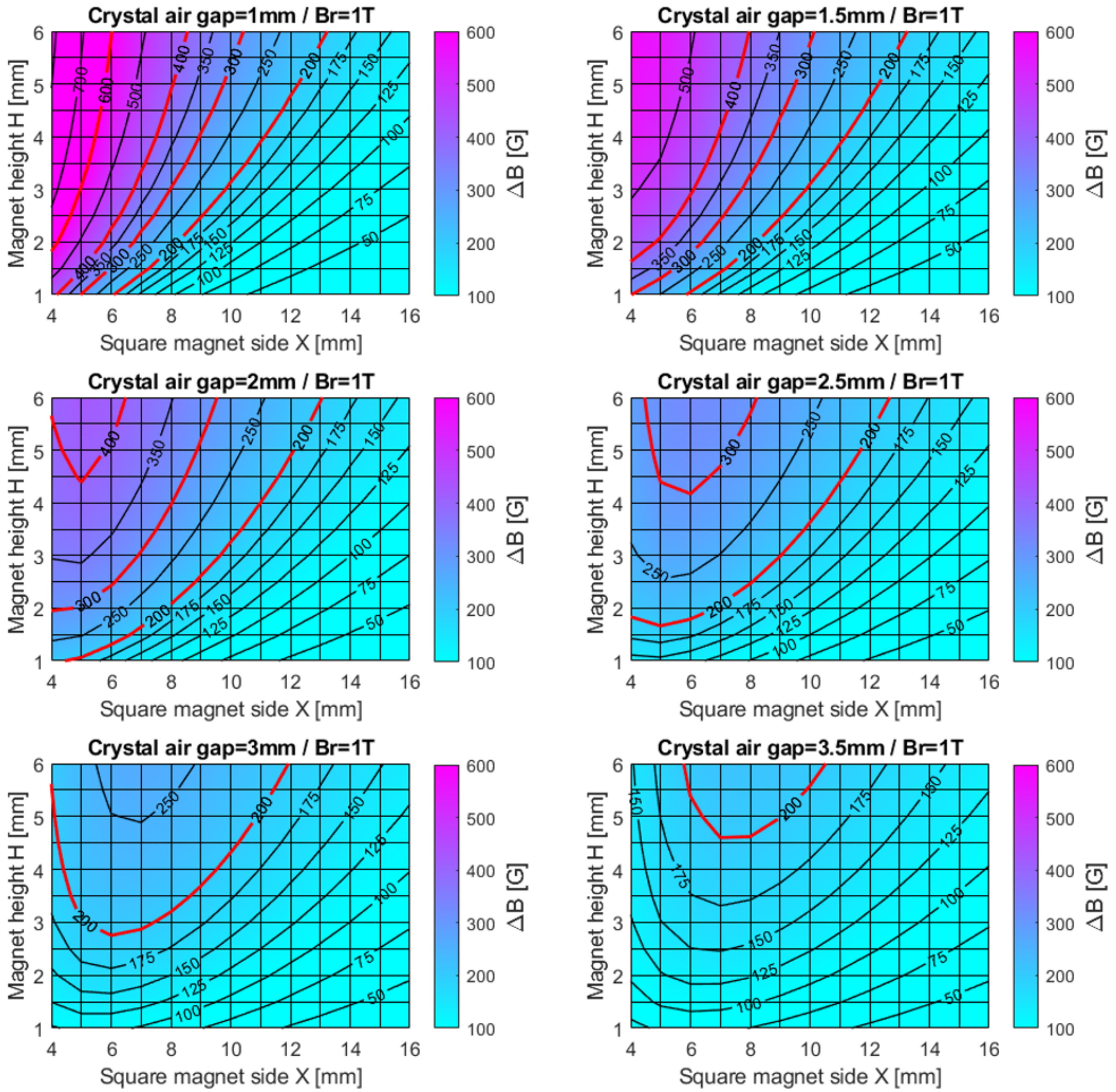

Figure 17: Square magnet, Differential input magnetic flux density with Br = 1 T and ideal A33020 placement versus the magnet

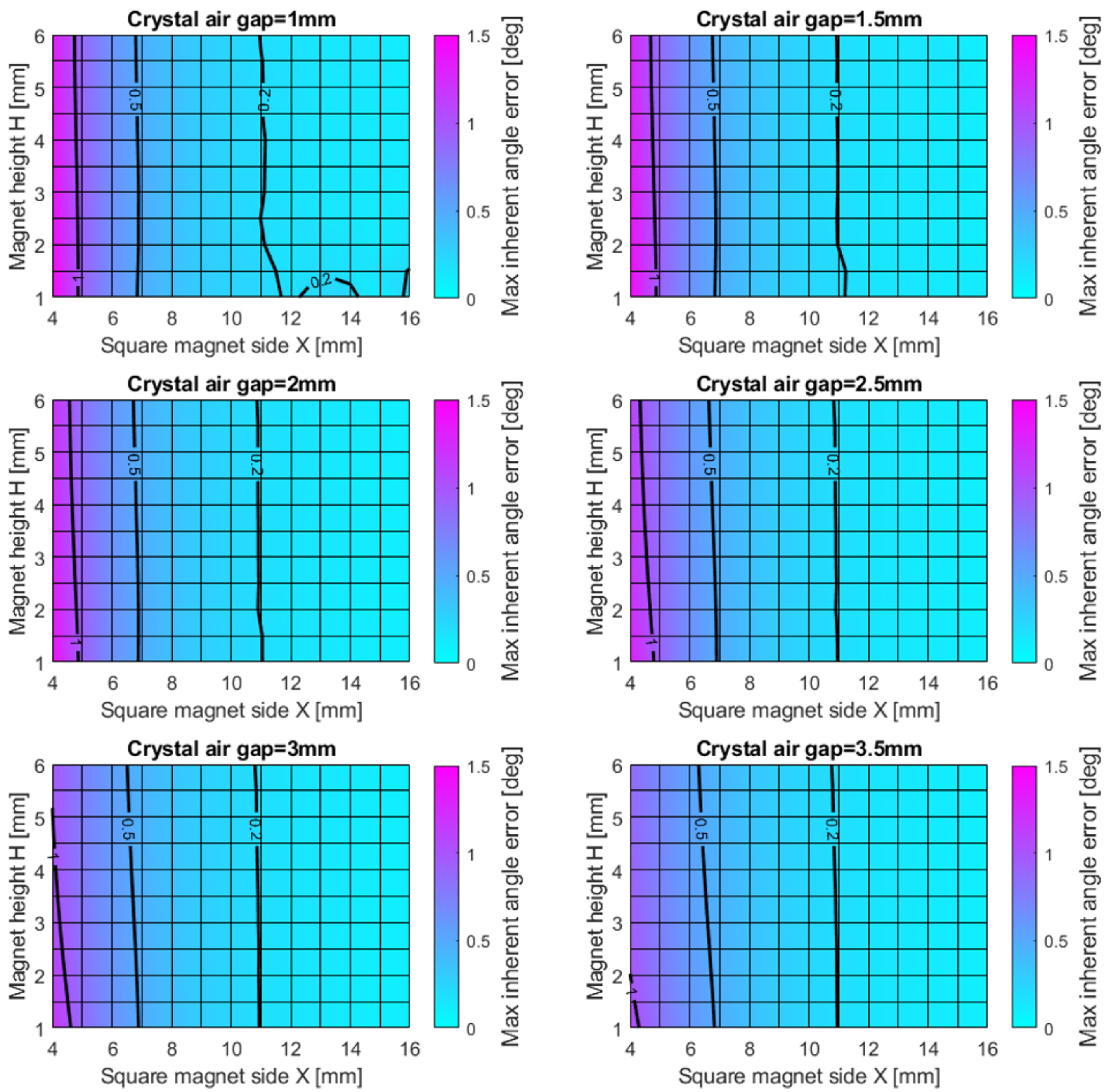

Figure 18: Square magnet, Maximum angle error over 360° with 0.5 mm in-plane A33020 misplacement versus the magnet

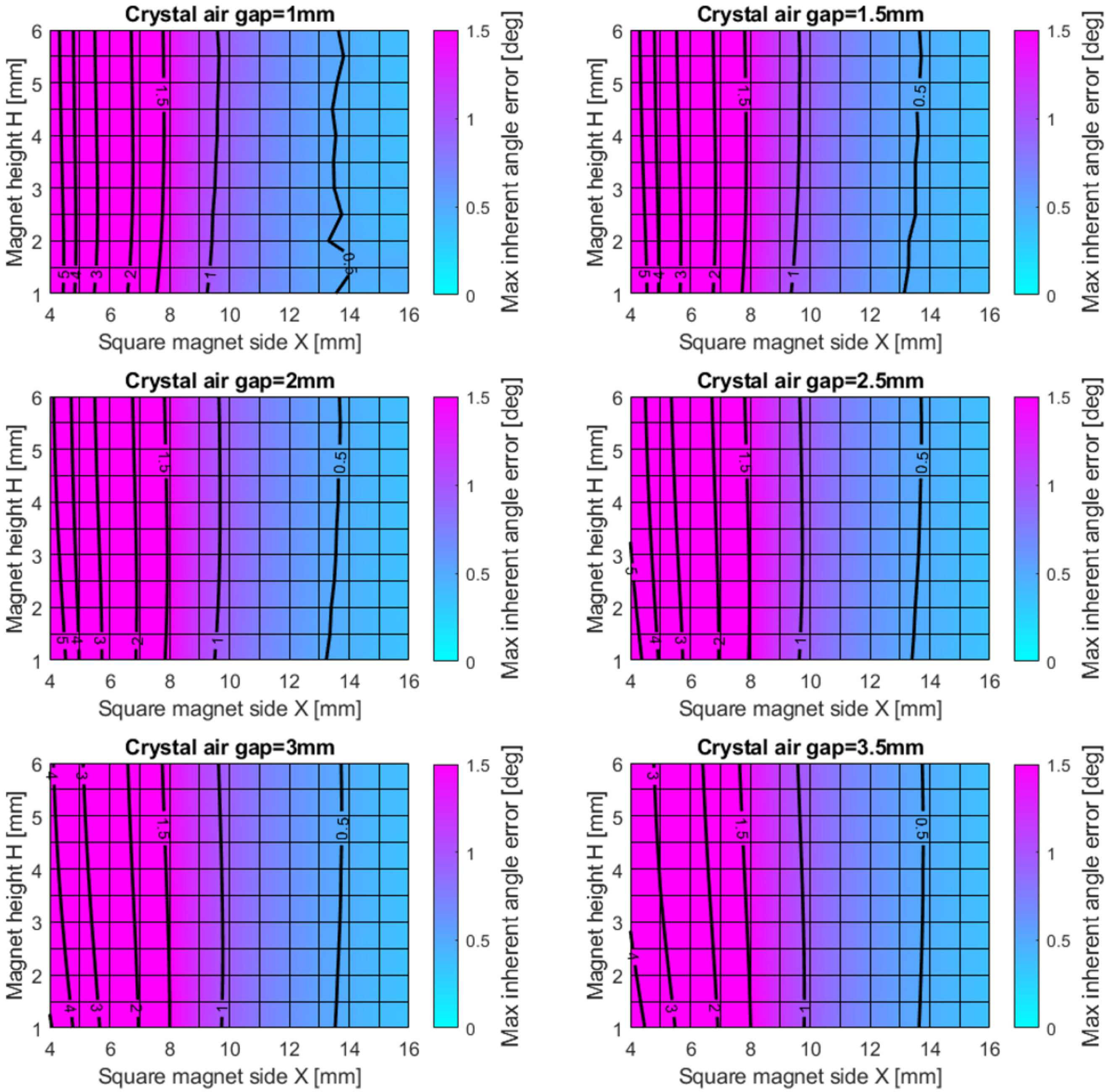

Figure 19: Square magnet, Maximum angle error over 360° with 1.0 mm in-plane A33020 misplacement versus the magnet

Revision History

Number	Date	Description
–	February 17, 2023	Initial release
1	March 21, 2023	Table 1 updated